Potential anti-HIV and antitrypanosomal components revealed in Sorindeia nitidula via LC-ESI-QTOF-MS/MS and molecular docking

Guy Roland Ebede
  University of Yaounde I

Emeka Emea Okoro
  Nottingham Trent University

Joséphine Ngo Mbing
  University of Yaounde I

Kolawole Ayodapo Olofinsan
  University of the Free State

Ochuko Lucky Erukainure
  University of Johannesburg

Patrick Hervé Diboue Betote
  Institute of Medical research and Medicinal Plants studies (IMPM)

Dieudonné Emmanuel Pegnyemb
  University of Yaounde I

Muhammad Iqbal Choudhary
  H.E.J. Research Institute of Chemistry, University of Karachi

Xavier Siwe-Noundou
  Sefako Makgatho Health Sciences University

Joseph Thierry Ndongo

  joseph.ndongo@univ-yaounde1.cm

  University of Yaounde I

Article

Keywords:

Additional Declarations: No competing interests reported.

Abstract

Sorindeia nitidula is used by traditional practitioners to treat influenza illnesses with cephalgia and febrile aches. However, the potential active ingredients for its remarkable antioxidant, anti-HIV and antitrypanosomal activities remain unexplored. The present study aims to evaluate the antioxidant, anti-HIV and antitrypanosomal activities of the ethyl acetate extract of *S. nitidula* (SN) in order to screen out the bioactive compounds and to analyze their possible mechanisms of action. Overall, 21 phenolic compounds were annotated, by using the MS and MS/MS information provided by the QTOF-MS. *In vitro* assays on the extract revealed potent antioxidant (IC$_{50}$ = 0.0129 mg/mL), anti-HIV (IC$_{50}$ = 1.736 mg/mL), antitrypanosomal (IC$_{50}$ = 1.040 μM) activities. Furthermore, SN did not present cytotoxic effect on HeLa cancer cell lines (IC$_{50}$ = 0.045 μM). Molecular docking revealed that the potential ligands exhibited strong binding ability and inhibitory activities on trypanosome. The integrated strategy based on LC-ESI-QTOF-MS/MS and molecular docking provided a powerful tool and a multidimensional perspective for further exploration of active ingredients in *S. nitidula* responsible for the antioxidant, anti-HIV and antitrypanosomal activities.

Introduction

The plant *Sorindeia nitidula* (SN) Engl., synonym of *Sorindeia africana* Engl. Van Der Veken is found throughout tropical Africa in tropical forests, gallery forests at altitudes reaching 1500 m and in thickets. It is also found in the wooded savannahs, dry forests, dense forests and humid regions of West and Central Africa, located north of the equator, more precisely in the Democratic Republic of Congo, Gabon and Cameroon. *Sorindeia nitidula* is known by several vernacular names in the Democratic Republic of Congo: Eloko loko, Inaolo an itende, Kasendo, Kassendu (turumbu) and Liembe (mongandu). In Cameroon, it has been identified in the western (Banganté and Mount Bamboutos), eastern (Bertoua) areas of the country[1]. It is used by traditional healers to treat influenza illnesses with cephalgia and febrile aches: the treatment consists of drinking the juice of the leaves, rubbing with the pulp and taking a steam bath with the decoction of barks[2]. *Sorindeia juglandifolia* from the same genus, have shown antiplasmodial activities and contain phenolic acids and flavonoids[3,4]. However, no previous anti-HIV and antitrypanosomal studies has been done on this genus.

Trypanosoma brucei gambiense and *Trypanosoma brucei rhodesiense* are two parasites, which, cause sleeping sickness, or human African trypanosomiasis (HAT) that is still endemic in well-defined regions of sub-Saharan Africa. Co-infections with human immunodeficiency virus (HIV) and HAT are not uncommon. Some studies have indicated that HIV-1 seropositive subjects may be at greater risk of HAT treatment failure and poor outcome than HIV-1 negative patients. However, the influence of HIV-1 on the epidemiology and/or clinical course of HAT remains unclear. This can be supported by the compromised immune system of the HIV patients[5,6]. Currently, there is no vaccine against HAT due to the antigenic variation exhibited by the parasites. Chemotherapy is mainly the mode of treatment centred on three key drugs; pentamidine for early-stage *T. brucei gambiense*, suramin for early-stage *T. brucei rhodesiense*, and melarsoprol for late-stage disease when trypanosomes are present in the central nervous system[7]. Likewise, mainly due to latency and quiescence inherent in the nature of the virus, presently, there is no cure or effective vaccine for the HIV disease. Despite the great success achieved so far with active antiretroviral therapy, sustainable control of the disease remains a significant challenge due to the continued emergence of cross-resistant viral strains and the associated adverse effects of most drugs on the patients. There is therefore an urgent need to discover new anti-HIV drug candidates and new antitrypanosomal treatments with minimal side effects, potency and pharmacokinetic profiles.

Some investigators reported that some medicinal plants exhibit anti-HIV and anti-trypanosome activity due to the presence of phenolic compounds[7–10]. Theses compounds are those that have an aromatic ring with at least one OH

group and whose structures can vary from simple phenols to complex polymers. According to the number of phenol units within the molecular structure, substituent groups, and the linkage type between phenol units, phenolic compounds can be classified into monomeric polyphenols, including phenolic acids, flavonoids (anthocyanins, flavanols, flavonols, flavanones, flavones, chalcones, and dihydroxy chalcones), stilbenes, and lignans, or polymeric polyphenols, such as tannins[11]. However, flavonoids are the most abundant phenolic compounds in nature[12]. Phenolic compounds are known to have strong antioxidant properties via different mechanisms, including scavenger of reactive oxygen species by transferring hydrogen atoms or donating electrons, oxidase inhibitors, metal chelators, and antioxidant enzyme cofactors[11]. To provide a better understanding of pharmacological functions of *S. nitidula* trunk, identification and characterization of bioactive compounds from *S. nitidula* trunk is essential. LC-MS/MS is an advanced and sophisticated technique that can be used to profile metabolites in a sample due to its high sensitivity, selectivity and high resolution. Additionally, this technique can reduce the complexity of metabolite samples by enabling the identification, measurement and separation of metabolites before their detection[13].

Given the limited knowledge of the molecular profile of *S. nitidula*, as well as the antiviral potential of natural products, herein we investigated the chemical diversity of extract from *S. nitidula*, *in vitro* antioxidant, anti-HIV and antitrypanosomal activities. Hence, we believe that this study of the chemical diversity and bioactivity properties of *S. nitidula* will lead to the discovery of promising candidates and support further research in the development of new anti-HIV and antitrypanosomal agents.

Methods

Chemicals and reagents

Analytical grade and pure (> 95%) solvents and chemicals were used in this study. Ultrapure deionized water (with resistivity 18.1 MX cm at 25°C), was acquired from Barnstead GenPure Water Purification System (Thermo Scientific, USA). Methanol was purchased from Merck KGaA, 64271 (Darmstadt, Germany), formic acid from Daejung (Daejung Chemicals and Metals Co. Ltd, Korea) Chemical and Metals (South Korea). Pharmaceutical Drugs standards ($\leq$ 98% purity) were obtained from the Drug Bank of Dr. Panjwani Center for Molecular Medicine and Drug Research (PCMD), International Centre for Chemical and Biological Sciences (ICCBS), University of Karachi, Karachi, Pakistan and from the Centre for Chemico and Biomedicinal Research (Rhodes University).

Sample collection and preparation of extract

The plant material (trunk) was collected at 10 km from Bagangte, going to Bankam Fokam, western region of Cameroon in January 2015. The sample collection was conducted following the guidelines and regulations of the legislation of Cameroon. The additional permission to collect and work on the plant *Sorindeia nitidula* was taken from the Forest Officer of the Range Forest Office Bangante, and from the Chief of village Bankam Fokam. Mr. Victor Nana, a botanist at National Herbarium of Cameroon in Yaoundé, identified the plant and the voucher specimen of *S. nitidula* (N° 26056/SRFCam) was deposited at the National Herbarium of Cameroon in Yaoundé.

The trunk of *S. nitidula* Engl. was dried at ambient temperature and far from sunlight, ground and 400 g of powder was obtained. Three hundred grams (300 g) of this powder were subjected to extraction with ethyl acetate (250 mL) by sonication using ultrasonic waves at a frequency of 50 kHz for 30 minutes. After filtration and evaporation of the filtrate to dryness using a rotary evaporator under vacuum (40 ºC, 60 rpm and a pressure of 200 mbar), an ethyl acetate extract of 10 g was obtained. Then, 1 g of the extract was dissolved in 10 mL of methanol and 1 mL supernatant was filtered through a syringe-driven PTFE filter (0.22 μm) into centrifuge tube (1.5 ml). For LC-MS analysis, the sample was transferred into HPLC vial, and twenty times diluted with methanol.

The remain EtOAc extract (5 g) was separated by column chromatography over silica gel (70−230 mesh; Merck), eluted with gradient solvent system of CH_2Cl_2/MeOH (100:0, 95:5, 90:10, 85:15, 80:20, 75:35, 70:30, 65: 35, 60:40, 50:50, 0:100, v/v). A total of 50 fractions of 250 mL each were obtained and combined based on TLC profiles into four main fractions (A−D). Fraction C (2.1 g, CH_2Cl_2/MeOH, 70:30, 65: 35 and 60:40) was subjected to column chromatography over silica gel (70−230 mesh; Merck), and eluted with CH_2Cl_2/MeOH: (10:1, 5:1, v/v) to yield methyl gallate (5 mg), and quercitrin (10 mg). Fraction D (30 mg, CH_2Cl_2/MeOH, 50:50 and 0:100) was purified by preparative HPLC (using MeOH/H_2O, 50/50, flow rate = 5 mL/min, t_R = 25 min, 35 min, and 40 min) to afford compounds quercetin (3 mg), eriodictyol (5 mg), and 3', 4', 5- trihydroxyflavone (7 mg), respectively. The mass and NMR spectra of these compounds are given in supporting files from Fig S18 to Fig S21.

Instrumentation and analytical conditions

In line with the protocols of the study, chemical fingerprinting of the EtOAc extract was performed using a high-resolution Bruker maXis-II QTOF Mass Spectrometer (Bremen, Germany) coupled to Thermofisher Ultimate 3000 series Ultra Performance Liquid Chromatography[14]. Macherey-Nagel C-18 column (3.0 x 50 mm, 1.8 mm particle size) was selected for chromatographic separation. Linear mobile phase gradient system was applied, consisting of type-I water as eluent (A) and methanol as eluent (B), with 0.1% formic acid as additive in both mobile phases. Solvent gradient was run as 40% B in 0.0 to 1.0 min, 50% B in 1.0 to 2.0 min, 60% B in 2.0 to 7.0 min, 80% B in 7.0 to 7.5 min, 90% B in 7.5 to 9.0 min and then again 40% B in 9.0 to 15.0 min. The overall run-time was 20 min including 0.5 min of column equilibration at the end. The constant solvent flowrate was set at 0.7 mL/min and 2 µL of each sample was injected through autosampler. The column was maintained at the temperature of 40°C[14]. Each experiment was accompanied with calibration using sodium formate solution (10 mM). Mass detection range was set between 50 and 1500 m/z. For positive ionization mode, 4500 V of capillary voltage was provided while drying gas (nitrogen) was flown at the rate of 10 mL/min with a temperature of 300°C. A smart strategy was designed for targeted and untargeted identification of metabolites. The targeted identification was done by generating a custom-made library of compounds reported from these plants. Bruker Daltonics Target Analysis 1.3 (Bremen, Germany) was used to screen the high-resolution mass spectra for these reported compounds by comparing accurate masses and isotopic patterns. The untargeted identification was performed by utilizing different ESI-MS/MS libraries such as Mass Bank of North America, NIST MS/MS libraries, and Mass Bank of Europe. All these libraries are easily accessible, and these libraries were incorporated in the NIST MS search system to make searching simple. The parameters like exact masses, isotopic patterns and MS/MS fragmentations were used for identification. The threshold value for high-resolution m/z matching was set under 5 ppm error and for isotopic matching, it was set under 50 mSigma value. DataAnalysis (version 4.4) was utilized to generate Extracted Ion Chromatograms (EIC) of each identified compound[14].

DPPH Radical Scavenging Assay

Ethanolic solution of 2, 2-diphenyl-1-picrylhydrazyl (DPPH) (95 µL, 300 µM) was mixed with the test solution (5 µL, 0.5 mg/ml), and kept at 37 ºC[15]. After 30 minutes, the absorbance was monitored at 517 nm by a microplate ELISA reader (P415384, SPECTRA Max, Molecular Devices, USA). The color of the solution faded from violet to pale yellow on reduction. Percent radical scavenging activity (% RSA) was determined by comparison with a DMSO containing control. The concentration of the test sample/extract that reduces 50% of the initial concentration of 2, 2-diphenyl-1-picrylhydrazyl (DPPH) is called IC_{50} value. The IC_{50} values of compounds were calculated by using EZ-Fit Enzyme Kinetics Software Program (Perrella Scientific Inc., Amherst, MA, USA). N-acetyl-L-cysteine was used as standard compound[16,17]. 2, 2-diphenyl-1-picrylhydrazyl (DPPH) free radical scavenging ability of flavonoid rich extract was calculated by using the Eq. (1).

$$DPPH\ inhibition\% = \frac{(Absorbance\ of\ Control - Absorbance\ of\ sample)}{Absorbance\ of\ control} \quad (1)$$

Trypanosoma brucei assay

To assess antitrypanocidal activity, *in vitro* cultures of *T. brucei* in 96-well plates were performed at a fixed concentration of 25 µg/mL for natural extract (unless otherwise stated)[18]. The number of parasites surviving drug exposure was determined by adding a resazurin based reagent, after an incubation period of 48 h[19]. The reagent contains resazurin which was reduced to resorufin by living cells. Indeed, resorufin is a fluorophore (Excitation 560/Emission 590) and can thus be quantified in a multiwell fluorescence plate reader[19].

HIV-1 integrase strand transfer reaction assay

Adaptation from previously described method helped to perform the HIV-1 subtype C integrase (CIN) strand transfer inhibition assay[7,20]. In summary, 20 nM double-stranded biotinylated donor DNA (5'-5 Biotin TEG/ACCCTTTTAGTCAGTGTGGAAAATCTCTAGCA-3' annealed to 5' ACTGCTAGAGATTTTCCACACTGACTAAAAG-3') was immobilised in wells of streptavidin coated 96-well microtiter plates (R&D Systems, USA). Following incubation at room temperature for 40 min and a stringent wash step, 5 µg/ml purified recombinant HIV- 1 CIN in buffer 1 (50 mm NaCl, 25 mM Hepes, 25 mM $MnCl_2$, 5 mM β-mercaptoethanol, 50 µg/ml BSA, pH 7.5) was added to individual wells. SN extract and chicoric acid were added to individual wells to a final concentration of 50 mg/ml (crude extract). Recombinant HIV-1 subtype C IN was assembled onto the preprocessed donor DNA through incubation for 45 min at room temperature[21]. Strand transfer reaction was initiated through the addition of 10 nM (final concentration) double-stranded FITC-labelled target DNA (5'-TGACCAAGGGCTAATTCACT/36-FAM/−3' annealed to 5'-AGTGAATTAGCCCTTGGTCA−/36-FAM/−3') in integrase buffer 2 (same as buffer 1, except 25 mm MnCl2 replaced with 2.5 mm $MgCl_2$). After an incubation period of 60 min at 37°C, the plates were washed using PBS containing 0.05% Tween 20 and 0.01% BSA, followed by the addition of peroxidase-conjugated sheep anti-FITC antibody (Thermo Scientific, USA) diluted 1:1000 in the same PBS buffer[20,21]. Finally, the plates were washed and peroxidase substrate (Sure Blue ReserveTM, KPL, USA) was added to allow for detection at 620 nm using a Synergy MX (BioTek®) plate reader. Absorbance values were converted to percentage enzyme activity relative to the readings obtained from control wells (enzyme without inhibitor) [7,21,22].

Cytotoxicity assay

This was adopted from our previously described method[7,21]. To assess the overt cytotoxicity, plant extract was incubated at 25 µg/ml in 96-well plates containing HeLa cells (Cellonex, Johannesburg, South Africa), maintained in a culture medium made of Dulbecco's Modified Eagle's Medium (DMEM) with 5 mM L-glutamine (Lonza, Basel, Switzerland) and supplemented with 10% fetal bovine serum (FBS) and antibiotics (penicillin/ streptomycin/fungizone - PSF) for 24 h. The resazurin based reagent and resorufin fluorescence was quantified (Excitation 560/Emission 590) in a multiwell plate reader and the number of cells surviving drug exposure were counted[21].

Single concentration screening and statistical analysis

The percentage of cell viability was calculated at a fixed concentration of 25 µg/ml for plant extract[20]. Experiments were performed in triplicate wells, and the standard deviation (SD) was derived. For comparative purposes, emetine (which induced cell apoptosis) or pentamidine (an existing drug used in the treatment of trypanosomiasis) were used as a positive control drugs standard.

Data were expressed as mean ± SEM. The statistical analyses of data were carried out using analysis of variance (ANOVA) followed by Turkey's test through GraphPad Prism 7.0 software. Significant difference was considered to P

value less than 0.05[22].

Molecular docking simulations

The 3D chemical structure of TryR, SOD, CP and PTR1 with respective access codes 2WPE, 3ESF, 2P7U and 3JQ6 were downloaded from the Protein Data Bank (PDB)[23]. The proteins were prepared for protein-ligand docking with the Dock prep tool of UCFS Chimera software V. 1.14[24]. Water and non-protein molecules attached to the proteins' crystallographic structure were removed before hydrogen atoms addition, protonation states and gasteiger charges[25]. The identified and isolated compounds, chemical structures in SDF format, retrieved from the PubChem website and optimized with Avogadro V1.2[26]. The active site location of each protein was determined with the CASTp online server before molecular docking was carried out with the AutodockVina algorithm[27]. The ligand docking with the protein targets was done using a search volume covering the catalytic pocket region. Then, the molecular interactions holding the protein-ligand complexes with the best binding pose for each enzyme were visualized with BIOVIA Discovery Studio[28].

Results and discussion

Chemical fingerprinting and identification of compounds

Chromatographic conditions were optimized for good shape and well separated peak. The overall runtime along with equilibration was kept within 20 min while the solvent flowrate was fixed at 0.7 mL/min. Mass fragmentation was performed on collision induced dissociation (CID) by varying the collision cell voltage. A total of fifteen-plant metabolites were identified by comparing accurate masses, fragmentation data and isotopic pattern (Table 1). *Sorindeia nitidula* showed seventeen peaks (Fig. 1) on extracting the total ion chromatogram (TIC) into base peak chromatogram (BPC). The MS/MS spectra of these compounds are given in supporting files from Fig S1 to Fig S17. Most of the identified compounds belong to phenolic acids, flavonoids and lignans classes of compounds (Fig. 2).

Table 1
Mass spectral characteristics and tentative identification of compounds

Peak	Retention time R.T (min)	Ion Molecular Formula (IMF) [M + H]$^+$	Theoretical (*m/z*)	Observed (*m/z*)	MS/MS Ions (% Intensity)	Tentative identification
Hydroxybenzoic acid derivatives						
4	9.85	C$_8$H$_9$O$_5$	185.0372	185.0332 [M + H]$^+$ 207.0138 [M + Na]$^+$	153.0090(100)	Methyl gallate
10	11.67	C$_{11}$H$_{11}$O$_9$	287.0398	287.0376 [M + H]$^+$ 309.0184 [M + Na]$^+$ 595.0482 [2M + Na]$^+$	153.0091(7), 241.0352(6), 269.0285(4), 287.0380(100)	2-*O*-Galloyl-L-malic acid
Hydroxycinnamic acid derivatives						
9	11.15	C$_{17}$H$_{17}$O$_4$	285.1132	285.1163 [M + H]$^+$ 307.0969 [M + Na]$^+$ 591.2066 [2M + Na]$^+$	149.1233(17), 177.1528(34), 201.0494(11), 229.0433(35), 247.2273(50), 265.2366(52), 285.1163(100)	Caffeic acid phenethyl ester
11	12.08	C$_{19}$H$_{19}$O$_8$	375.1002	375.0997 [M + H]$^+$ 397.0802 [M + Na]$^+$ 771.1735 [2M + Na]$^+$	146.0626(10),161.0851(100), 177.0667(7), 207.0754(20)	3-*O*-Methylrosmarinic acid
Flavanols						
1	9.18	C$_{15}$H$_{15}$O$_6$	291.0790	291.0689 [M + H]$^+$ 313,0496 [M + Na]$^+$ 603.1121 [2M + Na]$^+$	139.0306(100),147.0353(53), 165.0445(41), 179.0593(16), 205.0725(3), 207.0527(65), 249.0605(6), 273.0594(7)	(+)-Catechin

Peak	Retention time R.T (min)	Ion Molecular Formula (IMF) [M + H]+	Theoretical (*m/z*)	Observed (*m/z*)	MS/MS Ions (% Intensity)	Tentative identification
Hydroxybenzoic acid derivatives						
2	9.37	$C_{29}H_{23}O_{12}$	563.1195	563.1224 [M + H]+ 585.1032 [M + Na]+	165.0445(8), 231.0514(10), 272.0464(4), 393.0736(100), 423.0826(21)	7,4'-Di-*O*-Galloyltricetifavan
3	9.59	$C_{24}H_{21}O_{10}$	469.1056	469.1058 [M + H]+ 491.0869 [M + Na]+	153.0089(100), 221.0670(4), 245.0680(9), 297.0438(4), 433.0899(3)	Epigallocatechin-3-caffeate
6	10.11	$C_{22}H_{19}O_{10}$	443.0900	443.0709 [M + H]+ 465.0518 [M + Na]+ 907.1148 [2M + Na]+	153.0091(100), 165.0446(34), 188.0575(6), 207.0528(4), 231.0515(7), 255.0495(8), 273.0597(50), 291.0689(80)	Gallocatéchine-3-*O*-gallate
Flavone						
12	12.35	$C_{15}H_{11}O_5$	271.0528	271.0440 [M + H]+ 293.0248 [M + Na]+	271.0528(100),	Apigenin
13	13.39	$C_{25}H_{23}O_4$	387.1591	387.1568 [M + H]+ 409.1376 [M + Na]+	149.0147(43), 223.0500(37), 293.1715(46), 385.2693(100)	Fulvinervin B
14	13.69	$C_{25}H_{23}O_4$	387.1591	387.1573 [M + H]+ 409.1379 [M + Na]+ 795.2896 [2M + Na]+	147.0565(57), 163.0651(20), 185.0843(16), 207.0886(38), 267.1062(38), 293.1721(30), 337.1967(100), 385.2695(93)	Lineaflavone C
15	13.96	$C_{28}H_{25}O_{14}$	585.1093	585.1072 [M + H]+ 607.0880 [M + Na]+	168.9853(7), 227.0484(100), 256.2484(13), 285.0248(30), 327.2524(12), 371.2063(4), 553.0825(7)	Kaempferol galloyl deoxyhexosides
Flavanonol						

Peak	Retention time R.T (min)	Ion Molecular Formula (IMF) [M + H]$^+$	Theoretical (m/z)	Observed (m/z)	MS/MS Ions (% Intensity)	Tentative identification
Hydroxybenzoic acid derivatives						
8	10.89	$C_{15}H_{13}O_7$	305.0583	305.0474 [M + H]$^+$ 327.0281 [M + Na]$^+$ 631.0689 [2M + Na]$^+$	153.0091(65), 167.0240(15), 195.0171(19), 213.0416(6), 231.0515(83), 259.0447(100), 287.0380(22)	Taxifolin
Lignans						
7	10.41	$C_{22}H_{27}O_6$	387.1729	387.1779 [M + H]$^+$ 409.1593 [M + Na]$^+$ 795.3322 [2M + Na]$^+$	149.0875(34), 161.1231(16), 179.1311(6), 189.1156(24), 207.1254(100)	(+)-Eudesmin
16	14.25	$C_{27}H_{27}O_4$	415.1904	415.1890 [M + H]$^+$ 437.1675 [M + Na]$^+$	151.0872(17), 199.0999(3), 219.1615(15), 267.1071(100), 319.2650(33), 341.1751(16), 369.2285(25), 379.2612(11), 397.2214(19)	Simonsienol B
Other compounds						
5	9.96	$C_{45}H_{23}O_{25}$	963.0523	963.0525 [M + H]$^+$ 985.0345 [M + Na]$^+$	153.0091(100), 279.0335(23), 471.0260(9), 641.0386(3), 793.0411(27)	Unknown
17	15.04	$C_{26}H_{25}O_4$	385.1798	385.1798 [M + H]$^+$	170.0002(29), 184.0157(51), 255.1639(26), **269.1200**(43), 295.1773(23), 320.2077(21), 339.1770(100), 366.2112(24), 381.2394(91)	Unknown 4,4'-dimethoxychalcone derivative

Hydroxybenzoic acid derivatives

Benzoic acids and derivatives are also called benzenoids and are widely present in plants[12]. Two compounds were tentatively identified as hydroxybenzoic acid derivatives. Peaks 4 (t_R = 9.85 min) and 10 (t_R = 11.67 min) exhibited [M + H]$^+$ ions at m/z 185.0372 and 287.0398, respectively and showed identical fragmentation pattern as methyl gallate and 2-O-galloyl-L-malic acid. Further MS/MS analysis of the compounds showed fragment ion at m/z 153 that corresponded to loss of CH_3O for peak 4 and $C_4H_6O_5$ for peak 10 (malic acid) units[29].

Hydroxycinnamic acid derivatives

The hydroxycinnamic acids are the most abundant class of phenolic acids in fruits, herbs, and medicinal plants[12]. Two phenolic metabolites were identified as hydroxycinnamic acid derivatives in this selected plant. Peak 9 (t_R = 11.15 min) with [M + H]$^+$ at m/z 285.1163 gave origin to a fragment ion at m/z 177 [M − C$_8$H$_9$ − 2H]$^+$ by the simultaneous loss of the ethylbenzene ion and H$_2$ (in the precursor ion of caffeic acid). Its MS^2 profile also showed a distinct base peak with m/z 149 [M − C$_9$H$_9$O$_2$]$^+$ because of the removal of 4-vinylcatechol ion unit. Based on literature comparison, this compound was characterised as caffeic acid phenethyl ester (CAPE)[30]. The ESI-TOF-MS and MS/MS in the positive ion mode of peak 11 (t_R = 12.08 min) presented the molecular ion at m/z 375.0997 and base peak fragment at m/z 161. This fragmentation resulted from the deprotonated caffeoyl residue. Moreover, the *pseudomolecular* ion at m/z 375.0997 was in agreement with the rosmarinic acid derivative of published data[31]. As a result, peak11 was tentatively assigned as rosmarinic acid methyl ester.

Flavanols

Flavanols or favan-3-ols are also called monomeric flavanols including catechins, epicatechin, gallocatechin, epigallocatechin, and their gallate derivatives. They are the most common flavonoids due to their diversity in chemical structures and biological functions[12]. Four flavanols were tentatively identified in this study. Peak 1 (t_R = 9.18 min) exhibited [M + H]$^+$ ion at m/z 291.0689. The LC-MS/MS spectrum showed base peak at m/z 139, by loss of C$_8$H$_8$O$_3$ residue (m/z 152). In addition, the fragmented ion at m/z 273 resulted from a loss of water [M−18 + H]$^+$[32]. Hence, this compound was identified as + (−) catechin. Peak 6 (t_R = 10.11 min) was characterized as (+)-catechin 3-O-gallate based on the precursor ion [M + H]$^+$ at m/z 443.0709 and a major fragment peak ion at m/z 153 [M − 289]$^+$ due to loss of its aglycone, catechin observed in its LC-MS/MS spectrum. Two important product ions at m/z 273 [M − 169]$^+$ and 291 [M − 153 + 2H]$^+$ were also observed as in compound 1, which were attributable to loss of galloyl (C$_7$H$_5$O$_5$) and (3,4,5-trihydroxybenzylidyne) oxonium moieties, respectively (Zhu et al., 2022), from the precursor ion[11]. Peaks 2 (t_R = 9.37 min) and 3 (t_R = 9.59 min) were identified as 7,4'-di-O-galloyltricetifavan and epigallocatechin-3-caffeate based on the protonated molecular ions [M + H]$^+$ peaks at m/z 563.1224 and 469.1058, respectively. Theses identities were in agreement with previously reported literature and online databases[33,34]. The MS^2 spectrum produced ions at m/z 393 and 272 generated by the loss of a galloyl (− 169 Da) and C$_7$H$_5$O$_2$ (− 121 Da) moieties from the precursor aglycone of peak 2.

Flavones

In this context, four flavones were putatively identified in *S. nitidula* (Table 1). Peak 12 (t_R = 12.35 min) showing characteristic LC-MS spectrum and [M + H]$^+$ ion at m/z 271.0440 (Table 1) was identified as the flavone aglycone apigenin[35]. Peak 15 (t_R = 13.96 min) gave protonated ion at m/z 585.1072 and the MS^2 spectra showed product ions at m/z 285 that originated from the loss of a galloyl-deoxyhexosyl group[36]. The compound also exhibited diagnostic daughter ions for kaempferol and gallate at m/z 285, 256, 227 and 169 and thus, peak 15 was tentatively identified as kaempferol galloyl deoxyhexoside[37]. Peaks 13 (t_R = 13.39 min) and 14 (t_R = 13.69 min) were tentatively identified as fulvinervin B and lineaflavone C, respectively and presented [M + H]$^+$ ions at m/z 387.1568 and 387.1573[38,39]. MS^2 spectra of peaks 13 and 14 showed same fragments at m/z 385 [M − H]$^+$ and 293 [M − C$_6$H$_5$ − OH]$^+$ due to loss of hydrogen and consecutive losses of phenyl and hydroxyl groups, respectively. Peak 13 also exhibited diagnostic daughter ion for (*E*)-2, 2-dimethyl-8-(3-methylbuta-1,3-dien-1-yl)-*2H*-chromene at m/z 223 [M − C$_9$H$_6$O$_2$ − OH]$^+$. Moreover, the MS^2 of the peak 14 in the positive-ion mode was also dominated by ions losses at m/z 147 [M −

$C_{16}H_{16}O_2 + H]^+$, 267 $[M − C_8H_6 - OH]^+$, 337 $[M − 2xCH_3 − OH + 2H]^+$, which correspond to cleavage of the C ring and confirmed the presence of prenyl and dimethylpyran substituents (Supporting Information Fig. S14)[39].

Flavanonol

One flavanonol was detected in the *S. nitidula* extract. Thus, peak 8 (t_R = 10.89 min) was proposed as taxifolin (*m/z* 305.0474) in accordance with the MS/MS information.

The ions at *m/z* 287 $[M − H_2O + H]^+$ and 195 $[M − C_6H_5O_2]^+$ was due to the losses of a water molecule (− 18 Da) and catechol moiety, respectively[40]. MS^2 spectrum also showed daughter ions at *m/z* 153 and 167. The ion at *m/z* 153 correspond to cleavage of the C ring attributed to $^{1,3}B^-$ − 2H, and $^{1,3}A^-$ + 2H scissions, whereas at *m/z* 167 the ion corresponds to cleavage of the C ring attributed to $^{3,9}B^-$ − H scission[41].

Lignans

Lignans are a subgroup of non-flavonoid phenolic compounds, which comprise two phenylpropane units (C6−C3)[12]. They are commonly present in vegetables and fruits (Cassidy et al., 2000). These compounds can act as phytoestrogens as they have both hormonal and non-hormonal activities in animals[42]. Lignans have strong antioxidant and anti-diabetic capabilities with high medicinal value[43,44]. In this study, two lignans were tentatively identified. Peak 7 (t_R = 10.41min) with $[M + H]^+$ at *m/z* 387.1779 was identified as +(−) eudesmin, a non-phenolic furofuran lignan[45]. The MS^2 fragmentation showed the product ions at *m/z* 207 $[M − 179]^+$ and 179 $[M − 207]^+$, consistent with losses of 2-(2,4-dimethoxyphenyl) oxirenium and 2-(2,4-dimethoxyphenyl)tetrahydrofuran moieties, respectively after cleavage of furofuran ring. Daughter ions were also observed at *m/z* 189, 161 and 149 corresponding to the successive losses of CH_3, $2xOCH_3$ from the second and first moieties, respectively[46]. Peak 16, (t_R = 14.25 min) was identified with a signal peak at *m/z* 415.1890 in positive mode. MS^2 spectrum showed losses of 4-allylbenzene-1,3-diol ($C_9H_9O_2$) and magnolol ($C_{18}H_{17}O_2$) derivatives ions at *m/z* 267 $[M − 147]^+$ and 151 $[M − 265]^+$, respectively. The observation of other fragments associated with losses at *m/z* 397 $[M − 17]^+$, 379 $[M − 2x18 + H]^+$ and 341$[M − 2x17−41 + 2H]^+$ confirmed the presence of hydroxyl and allyl groups in the structure. Hence, compound 17 was identified as simonsienol B, a sesquilignan[47]. To our best knowledge, the lignans identified in our study were the first time detected by LC-MS/MS in the *Sorindeia* genus.

Unknown Compounds

Peak 4 was detected at m/z 963.0525 $[M + H]^+$ but not identified. Peak 17 with a parent ion at *m/z* 385.1798 $[M + H]^+$ which yielded product ion at *m/z* 269.1200 (4,4'-dimethoxychalcone), was identified as an unknown 4,4'-dimethoxychalcone derivative[48].

DPPH radical scavenging activity

DPPH radical is one of the free radicals widely used for testing the preliminary radical scavenging activity of the plant extract, as it is a direct and reliable method for determining radical scavenging activity[49]. Crude extract of *S. nitidula* was evaluated for their antioxidant activity comparing with the standard N-acetyl-L-cysteine. The results are presented in Table 2. The whole plant extract fraction showed 94.9% radical scavenging activity, as compared to the standard, N-acetyl-L-cysteine, that showed 97.5% RSA. In general, the phenolic compounds are one of the contributors to the antioxidant activities. Polyphenols have significant antioxidant effects, which can reduce oxygen free radicals in the human body, inhibit oxidative stress, and play a role in anti-aging, liver protection, neuroprotection, and anti-atherosclerosis [49]. Hydroxyl group in the ring of flavonoids have significant role in antioxidant activity since it donates

a hydrogen atom to stabilize the free radicals. Thus, screening of these phenolic compounds is essential. The abundant presence of methyl gallate (MG) and catechins on the extract can also explain the good activity of the extract. MG derived from natural plant sources exhibits high antioxidant activity, making it a valuable natural source of antioxidants[50]. Catechins possess significant antioxidant effects and strong activity against several pathogens, including bacteria, viruses, parasites, and fungi[51].

Table 2. *In vitro* assays of the ethyl acetate extract.

Sample	Antioxidant IC$_{50}$ (mg/ml)	Antitrypanosomal IC$_{50}$ (μM)	Cytotoxicity IC$_{50}$ (μM)	Anti-HIV IC$_{50}$ (μM)
SN[a]	0.0129	1.040	-	1.736
Reference drug[b]	0.0141	0.000782	0.045	0.008099
IC$_{50}$: 50% inhibitory concentration, i.e. the concentration of extract that reduces by 50% the growth or proliferation of cells.				
The number of replicates was 3.				
[a] (SN) ethyl acetate extract of *Sorindeia nitidula* trunk.				
[b] Reference drugs, i.e. N-acetyl-L-cysteine, pentamidine, emetine and L-chicoric acid for antioxidant, antitrypanosomal, cytotoxicity and HIV-1 IN activities, respectively used at a concentration of 0.5 mg/ml for the first drug or at 25 μg/ml in case of the three second drugs.				

Antitrypanosomal activity

The ethyl acetate extract from *S. nitidula* trunk (SN) affected the growth of trypanosomes at 25 μg/mL concentration with a percentage of viable parasites estimated to be 4.68 ± 0.56% (Fig. 4). Furthermore, SN extract was both in the lower range of IC$_{50}$ value (1.040 μM), whereas the reference drug pentamidine exhibited an IC$_{50}$ value of 0.000782 μM (Table 2). The plant has not been previously used as antitrypanosomial treatment in traditional Cameroonian medicine and there is not information available on the antitrypanosomal effects of the genus *Sorindeia*. The crude extract SN contain flavonoids that may be responsible for the antitrypanosomial activity in the *S. nitidula* species, as showed in the LC-MS/MS results. According to Vigueira et al., epigallocatechin-3-gallate is an active polyphenol compound against *Trypanosoma brucei*[9].

Cytotoxic activity

The ethyl acetate extract from *S. nitidula* trunk (SN) did not show cytotoxic activity against HeLa cells. Indeed, the extract was not cytotoxic at 25 μg/ml, giving 64.68 ± 0.43% of viability whereas the reference drug emetine exhibited an IC$_{50}$ value of 0.045 μM (Table 2).

Finally, as SN extract showed substantial antioxidant and antitrypanosomal activities without toxicity on HeLa cells, this suggested that the effects on parasite cultures may not arise from a general cytotoxic effect of the crude extract.

Anti-HIV IN assay

The *S. nitidula* ethyl acetate crude extract was tested and exhibited activity against HIV-1 IN (Fig. 5). The IC_{50} of the crude extract was found to be 1.736 μM. Interestingly, the IC_{50} of L-chicoric acid was found to be higher (IC_{50} = 0.008099 μM). The methyl gallate isolated and identified might be the principle chemical constituent that is responsible for the anti-HIV IN activity of the ethyl acetate *S. nitidula* trunk extract. It was showed that, methylgallate inhibits HIV-1 IN by chelating the active site Mg^{2+} cofactor.[7]

Molecular modeling study

As shown in Table 3, molecular docking studies revealed potent molecular interactions of the isolated compounds with trypanothione reductase (TryR), Fe-superoxide dismutase from *Trypanosoma brucei* (SOD), and cysteine protease (CP), pteridine reductase 1 (PTR1). Fulvinervin B showed the most potent molecular interaction with TryR, with a free binding energy of 9 kcal/mol (Fig. 3A). For SOD, CP and PTR1, 7,4'-Di-*O*-Galloyltricetifavan displayed the most potent molecular interaction, with free binding energies of -10.6, -8.5 and − 9.7 kcal/mol, respectively (Figs. 3B-3D). The inhibition of these enzymes in *Trypanosoma brucei* have been reported as a major antitrypanosomial mechanism[52−55]. The molecular interactions also corroborate the antitrypanosomial activity of *S. nitidula* extract, and may be attributed to the synergistic effect of the compounds.

Table 3

The free binding energy (kcal/mol) of *Sorindeia nitidula* extract phytochemicals with various protein targets

Compound	TryR	SOD	CP	PTR1
Quercitrin	-7.9	-9.3	-7.1	-9.1
Quercetin	-8.0	-8.2	-7.3	-8.4
Eriodictyol	-8.0	-8.4	-6.8	-8.3
3', 4', 5- trihydroxyflavone	-7.2	-9.5	-7.4	-9.4
Methyl gallate	-6.3	-5.7	-5.1	-5.5
Catechin	-7.6	-7.9	-6.7	-8.6
7,4'-Di-*O*-Galloyltricetifavan	-8.1	**-10.6**	**-8.5**	**-9.7**
Epigallocatechin-3-caffeate	-7.7	-10.0	-6.5	-9.6
Gallocatéchine-3-*O*-gallate	-7.2	-9.9	-7.9	-9.2
Eudesmin	-6.3	-8.2	-6.3	-8.3
Taxifolin	-7.9	-7.9	-7.0	
Caffeic acid phenethyl ester	-8.2	-7.1	-6.2	-8.3
2-*O*-Galloyl-L-malic acid	-6.6	-6.7	-5.6	-7.1
3-*O*-Methylrosmarinic acid	-7.2	-8.2	-6.7	-8.0
Apigenin	-8.3	-8.3	-7.0	-8.0
Fulvinervin B	**-9.0**	-9.6	-7.5	-9.4
Values in bold represent the binding energy of compound with the highest affinity for each protein				

Conclusion

The LC-MS/MS study of active fraction from *S. nitidula* led to the identification of seventeen phenolic derivatives compounds, reported from this species for the first time. The current studies also showed that *S. nitidula* is a natural source for flavonoids and hydroxybenzoic acids with potent free radical scavenging activity. The antitrypanosomal activity exhibited in this study could be ascribed to the presence of certain flavonoids identified in the trunk, but it would be interesting to establish whether these compounds are also present in the leaves as they may be used interchangeably or in conjunction with the leaves for the treatment of the mentioned trypanosomial infections.

Data availability

The data that support the fndings of this study are available in the supplementary material of

this article.

Declarations

Competing Interests

The authors declare no competing interests.

Author Contribution

G.R.E. conceived and designed the study. Conceptualization, methodology, writing original draft, editing and visualization was done by G.R.E., E.E.O. and X.S.N. X.S.N performed the in vitro assays. P.H.D.B. has drawn figures of the in vitro assays. K.A.O and O.L.E. performed docking experiments. Supervision, review and editing was done by J.T.N, J.N.M., D.E.P. and M.I.C. G.R.E., J.T.N. and X.S.N.wrote the final manuscript.

Acknowledgments

Data availability

The authors confirm that the data supporting the findings of this study are available within the article and its supplementary information.

References

1. Breteler, F. J. The African genus *Sorindeia* (Anacardiaceae): a synoptic revision. Adansonia. 25, 93–113 (2003).
2. Bouwet, A. Féticheurs et médecines traditionnelles du congo (brazzaville). Paris: Office de la Recherche Scientifique et Technique Outre-Mer (O.R.S.T.O.M.). 55 (1960)
3. Ndongo, J. T. *et al*. A new C-Glucosylflavone from *Sorindeia juglandifolia*. Z. Naturforsch. C. 68, 169–174 (2013).
4. Kamkumo, R. G. *et al*. Compounds from *Sorindeia juglandifolia* (Anacardiaceae) exhibit potent anti-plasmodial activities *in vitro* and *in vivo*. Malar J. 11, 1–7 (2013).
5. Barat, C., Pepin, J., & Tremblay, M. J. HIV-1 replication in monocyte-derived dendritic cells is stimulated by melarsoprol, one of the main drugs against human African trypanosomiasis. J Mol Biol. 410, 1052–1064 (2011).
6. Camacho, M. D. R. *et al*. *In vitro* activity of *Triclisia* patens and some bisbenzylisoquinoline alkaloids against *eishmania donovani* and *Trypanosoma brucei brucei*. *Phytother Re*. 16, 432–436 (2002).
7. Siwe-Noundou, X. *et al*. Anti-HIV-1 integrase potency of methylgallate from *Alchornea cordifolia* using *in vitro* and in silico approaches. Sci Rep. 9, 4718 (2019).
8. Larit, F. *et al*. Proposed mechanism for the antitrypanosomal activity of quercetin and myricetin isolated from *Hypericum afrum* Lam.: Phytochemistry, *in vitro* testing and modeling studies. *Molecules*. 26, 1009 (2021).
9. Vigueira, P. A., Ray, S. S., Martin, B. A., Ligon, M. M., & Paul, K. S. Effects of the green tea catechin (−)-epigallocatechin gallate on *Trypanosoma brucei*. Int J Parasitol.: Drugs Drug Resist. 2, 225–229 (2012).

10. Amisigo, C. M., Antwi, C. A., Adjimani, J. P. & Gwira, T. M. *In vitro* anti-trypanosomal effects of selected phenolic acids on *Trypanosoma brucei*. PLoS One. 14, e0216078 (2019).

11. Zhu, Z. *et al*. Lc-esi-qtof-ms/ms characterization and estimation of the antioxidant potential of phenolic compounds from different parts of the lotus (*nelumbo nucifera*) seed and rhizome. ACS omega. 7, 14630–14642 (2022).

12. Ali, A., Cottrell, J. J. & Dunshea, F. R. Lc-ms/ms characterization of phenolic metabolites and their antioxidant activities from australian native plants. Metabolites. 12, 1016 (2022).

13. Rafi, M. *et al*. LC-MS/MS based metabolite profiling and lipase enzyme inhibitory activity of *Kaempferia angustifolia* Rosc. with different extracting solvents. Arab. J. Chem. 15, 104232 (2022).

14. Shadab, H. *et al*. Cross-mixing study of a poisonous Cestrum species, *Cestrum diurnum* in herbal raw material by chemical fingerprinting using LC-ESI-QTOF-MS/MS. Arab. J. Chem. 13, 7851–7859 (2020).

15. Kumar, S. S., Krishnakumar, K. & John, M. Flavonoids from the butanol extract of Carica papaya L. cultivar'Red Lady'leaf using UPLC-ESI-Q-ToF-MS/MS analysis and evaluation of the antioxidant activities of its fractions. Food Chem. Adv. 1, 100126 (2022).

16. Uttara, B., Singh, A. V., Zamboni, P. & Mahajan, R. T. Oxidative stress and neurodegenerative diseases: a review of upstream and downstream antioxidant therapeutic options. Curr. Neuropharmacol. 7, 65–74 (2009).

17. Thadhani, V. M. *et al*. Antioxidant activity of some lichen metabolites. Nat Prod Res. 25, 1827–1837 (2011).

18. Eze, F. I., Noundou, X. S., Osadebe, P. O. & Krause, R. W. Phytochemical, anti-inflammatory and anti-trypanosomal properties of *Anthocleista vogelii* Planch (Loganiaceae) stem bark. J. Ethnopharmacol. 238, 111851 (2019).

19. Teinkela, J. E. M. *et al*. Biological activities of plant extracts from *Ficus elastica* and *Selaginella vogelli*: An antimalarial, antitrypanosomal and cytotoxity evaluation. Saudi J. Biol. Sci. 25, 117–122 (2018).

20. Grobler, J. A. *et al*. Diketo acid inhibitor mechanism and HIV-1 integrase: implications for metal binding in the active site of phosphotransferase enzymes. Proc Nat Acad Sci U.S.A. 99, 6661–6666 (2002).

21. Siwe-Noundou, X. *et al*. Biological activity of plant extracts and isolated compounds from Alchornea laxiflora: Anti-HIV, antibacterial and cytotoxicity evaluation. S Afr J Bot. 122, 498–503 (2019).

22. Djouwoug, C. N. *et al*. *In vitro* and *in vivo* antiplasmodial activity of hydroethanolic bark extract of *Bridelia atroviridis* müll. Arg.(Euphorbiaceae) and lc-ms-based phytochemical analysis. *J. Ethnopharmacol*. 266, 113424 (2021).

23. Salau, V. F. *et al*. Vanillin improves glucose homeostasis and modulates metabolic activities linked to type 2 diabetes in fructose–streptozotocin induced diabetic rats. Arch. Physiol. Biochem. 1–14 (2021).

24. Pettersen, E. F. *et al*. UCSF Chimera—a visualization system for exploratory research and analysis. J Comput Chem. 25, 1605–1612 (2004).

25. Wang, J., Wang, W., Kollman, P. A. & Case, D. A. Automatic atom type and bond type perception in molecular mechanical calculations. J Mol Graph Model. 25, 247–260 (2006).

26. Hanwell, M. D. et al. Avogadro: an advanced semantic chemical editor, visualization, and analysis platform. J cheminformatics. 4, 1–17 (2012).

27. Trott, O. & Olson, A. J. AutoDock Vina: improving the speed and accuracy of docking with a new scoring function, efficient optimization, and multithreading. J Comput Chem. 31, 455–461 (2010).

28. Systèmes, D. Biovia, discovery studio modeling environment. Dassault Systèmes Biovia: San Diego, CA, USA. (2016).

29. Abu-Reidah, I. M., Ali-Shtayeh, M. S., Jamous, R. M., Arráez-Román, D. & Segura-Carretero, A.. HPLC–DAD–ESI-MS/MS screening of bioactive components from *Rhus coriaria* L.(Sumac) fruits. Food chem. 166, 179–191

(2015).

30. Tang, C. & Sojinu, O. S. Simultaneous determination of caffeic acid phenethyl ester and its metabolite caffeic acid in dog plasma using liquid chromatography tandem mass spectrometry. Talanta. 94, 232–239 (2012).

31. Lee, Y. H. *et al*. Characterization of metabolite profiles from the leaves of green perilla (*Perilla frutescens*) by ultra high performance liquid chromatography coupled with electrospray ionization quadrupole time-of-flight mass spectrometry and screening for their antioxidant properties. J Food Drug Anal. 25, 776–788 (2017).

32. Chang, C. L. & Wu, R. T. Quantification of (+)-catechin and (−)-epicatechin in coconut water by LC–MS. Food chem. 126, 710–717 (2011).

33. Li, Y., Leung, K. T., Yao, F., Ooi, L. S. & Ooi, V. E. Antiviral flavans from the leaves of *Pithecellobium c lypearia*. J Nat Prod. 69, 833–835 (2006).

34. Umehara, M., Yanae, K., Maruki-Uchida, H. & Sai, M. Investigation of epigallocatechin-3-*O*-caffeoate and epigallocatechin-3-Op-coumaroate in tea leaves by LC/MS-MS analysis. Food Res Int. 102, 77–83 (2017).

35. Brito, A., Ramirez, J. E., Areche, C., Sepúlveda, B. & Simirgiotis, M. J. HPLC-UV-MS profiles of phenolic compounds and antioxidant activity of fruits from three citrus species consumed in Northern Chile. Molecules. 19, 17400–17421 (2014).

36. Gu, D. *et al*. A LC/QTOF−MS/MS application to investigate chemical compositions in a fraction with protein tyrosine phosphatase 1B inhibitory activity from *Rosa rugosa* flowers. Phytochem. Anal. 24, 661–670 (2013).

37. Li, C. & Seeram, N. P. Ultra-fast liquid chromatography coupled with electrospray ionization time-of-flight mass spectrometry for the rapid phenolic profiling of red maple (*Acer rubrum*) leaves. J Sep Sci. 41, 2331–2346 (2018).

38. Dawande, V. R. & Gurav, R. V. Qualitative analysis of phytochemical in *Eulophia nuda* using LCMS. J Med Plants Stud. 9, 136–140 (2021).

39. Owor, R. O. *et al*. Anti-inflammatory flavanones and flavones from *Tephrosia linearis*. J Nat Prod. 83, 996–1004 (2020).

40. Taamalli, A. *et al*. LC-MS-based metabolite profiling of methanolic extracts from the medicinal and aromatic species *Mentha pulegium* and *Origanum majorana*. Phytochem. Anal. 26, 320–330 (2015).

41. Escobar-Avello, D. *et al*. Phenolic profile of grape canes: Novel compounds identified by lc-esi-ltq-orbitrap-ms. Molecules. 24, 3763 (2019).

42. Cassidy, A., Hanley, B. & Lamuela-Raventos, R. M. Isoflavones, lignans and stilbenes – origins, metabolism and potential importance to human health. J Sci Food Agric. 80, 1044–1062 (2000).

43. Chen, Z., Zhong, B., Barrow, C. J., Dunshea, F. R. & Suleria, H. A. Identification of phenolic compounds in Australian grown dragon fruits by LC-ESI-QTOF-MS/MS and determination of their antioxidant potential. Arab J Chem. 14, 103151(2021).

44. Ebede, G. R. *et al*. Isolation of new secondary metabolites from the liana *Landolphia lucida* K. Schum. (Apocynaceae). Phytochem Lett. 41, 27–33 (2021).

45. Jaiswal, Y., Liang, Z., Ho, A., Chen, H. & Zhao, Z. Metabolite profiling of tissues of *Acorus calamus* and *Acorus tatarinowii* rhizomes by using LMD, UHPLC-QTOF MS, and GC-MS. Planta Med. 81, 333–341(2015).

46. Katchborian, N. A. Biomarkers of anti-inflammatory and neuroprotective activity investigated by untargeted UPLC-ESI-QTOF-MS metabolomics analyses.123f. Dissertação ((Mestrado em Química) - Universidade Federal de Alfenas, Alfenas/MG. 80, 108 (2020)

47. Dong, C. F. *et al*. Sesquilignans and sesquiterpenoid from the stem barks of *Illicium simonsii* and their anti-AChE activity. Nat Prod Bioprospecting. 2, 133–137 (2012).

48. Wang, Y., Cheng, J., Jiang, W. & Chen, S. Metabolomics study of flavonoids in *Coreopsis tinctoria* of different origins by UPLC−MS/MS. PeerJ. 10, e14580 (2022).

49. Sulaiman, C. T. & Balachandran, I. LC/MS characterization of antioxidant flavonoids from *Tragia involucrata* L. Beni-Suef Univ J Basic App Sci. 5, 231−235 (2016).

50. Liang, H. *et al*. Methyl gallate: Review of pharmacological activity. Pharmacol Res. 106849 (2023).

51. Geana, E. I. *et al*. Antioxidant and Wound Healing Bioactive Potential of Extracts Obtained from Bark and Needles of Softwood Species. Antioxidants. 12, 1383 (2023).

52. Ettari, R. *et al*. The inhibition of cysteine proteases rhodesain and TbCatB: A valuable approach to treat Human African Trypanosomiasis. Mini-Rev Med Chem. 16, 1374−1391 (2016).

53. Prathalingham, S. R., Wilkinson, S. R., Horn, D. & Kelly, J. M. Deletion of the *Trypanosoma brucei* superoxide dismutase gene sodb1 increases sensitivity to nifurtimox and benznidazole. Antimicrob Agents Chemother. 51, 755−758 (2007).

54. Richardson, J. L *et al*. Improved tricyclic inhibitors of trypanothione reductase by screening and chemical synthesis. ChemMedChem. 4, 1333−1340 (2009).

55. Wang, J., Wang, W., Kollman, P. A. & Case, D. A. Automatic atom type and bond type perception in molecular mechanical calculations. J Mol Graph Model. 25, 247−260 (2006).
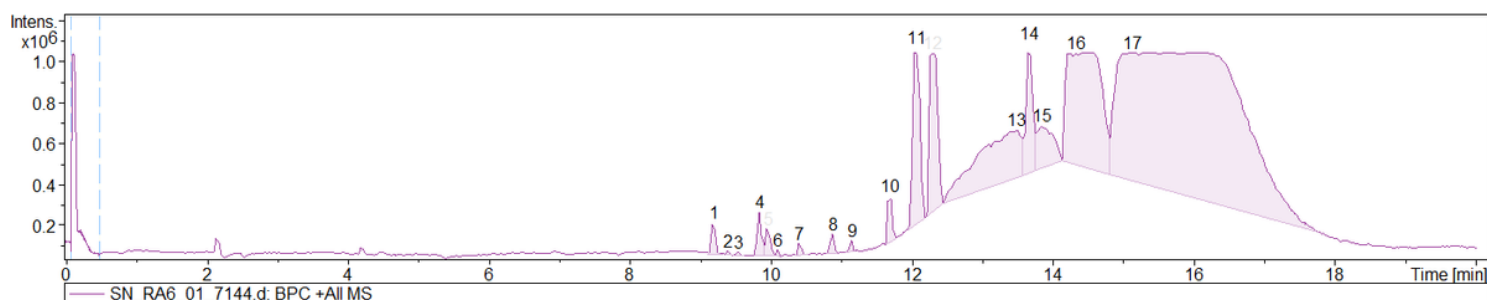
Figures

Figure 1

MS base peak chromatogram (bpc) of *sorindeia nitidula*.

(+)-Catechin

(+)-Eudesmin

Caffeic acid phenethyl ester

3-*O*-Methylrosmarinic acid

Taxifolin

Apigenin

Fulvinervin B

Lineaflavone C

Simonsienol B

Epigallocatechin-3-caffeate

Gallocatéchine-3-*O*-gallate

Methyl gallate

7,4'-Di-*O*-Galloyltricetifavan

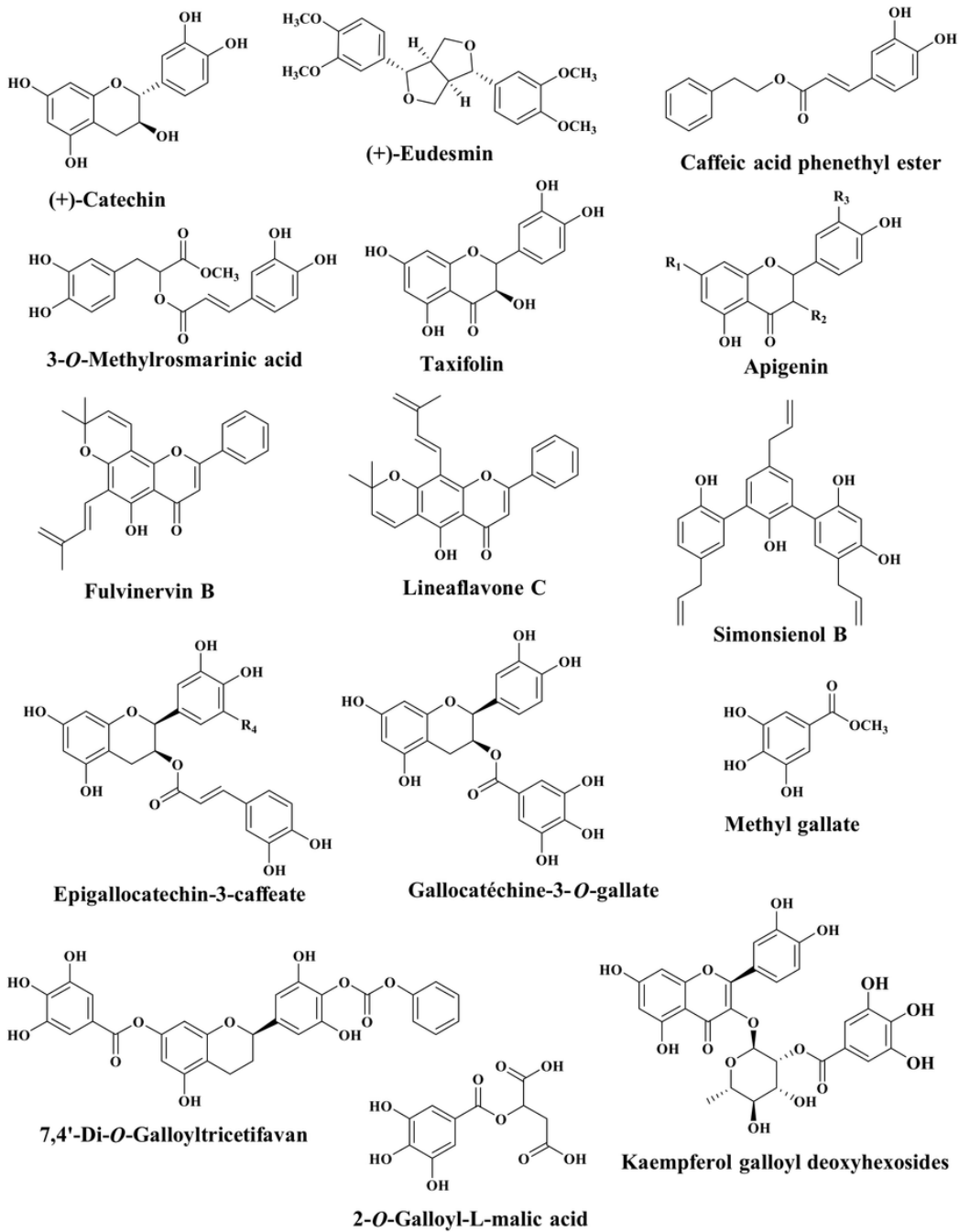2-*O*-Galloyl-L-malic acid

Kaempferol galloyl deoxyhexosides

Figure 2

structures of identified and isolated compounds from the ethylacetate extract of *sorindeia nitidula* engl. (Anacardiaceae).
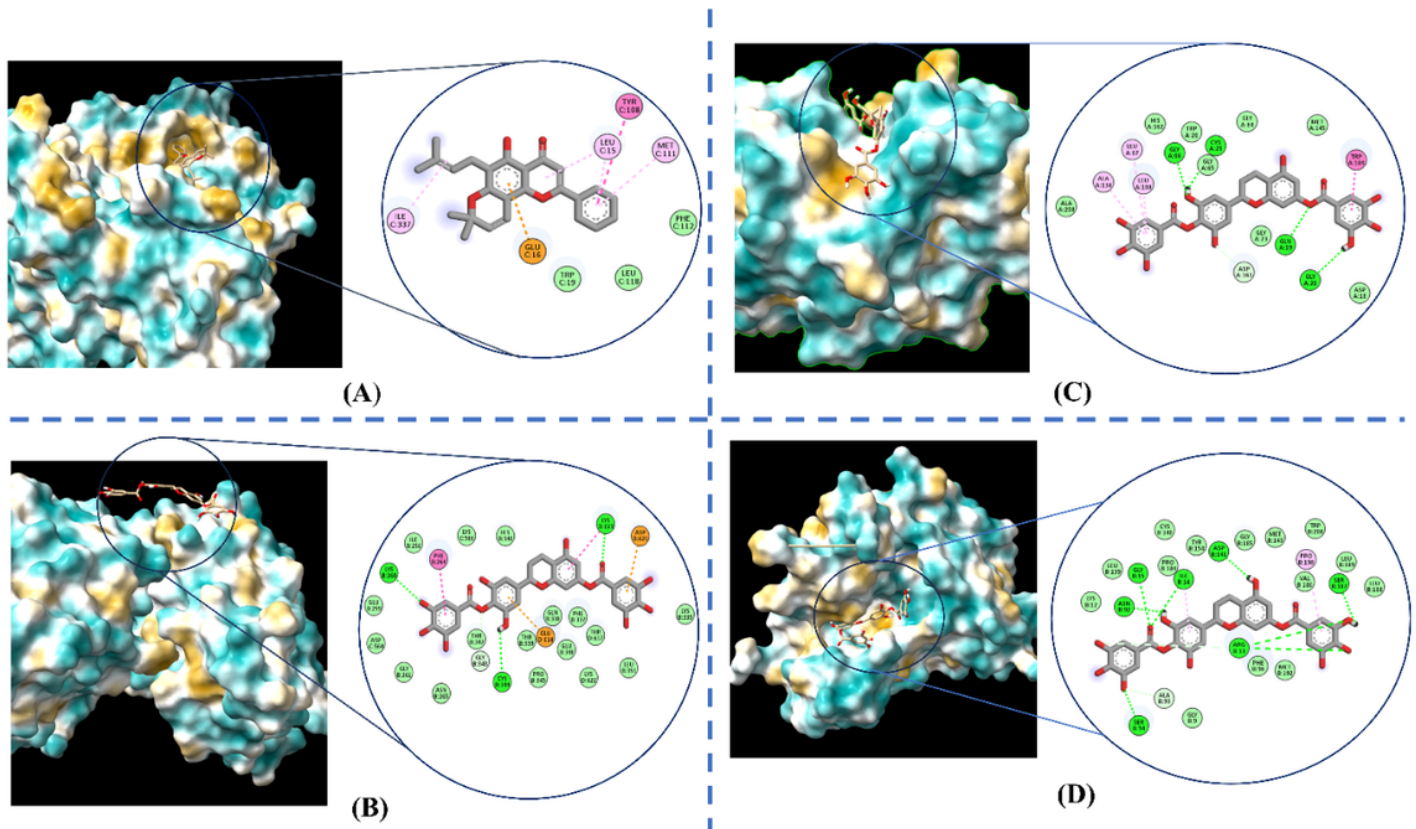
Figure 3

Images of active site interactions between (A) fulvinervin B and tryr (B) 7,4'-di-*o*-galloyltricetifavan and sod (C) 7,4'-di-*o*-galloyltricetifavan and cp (D) 7,4'-di-*o*-galloyltricetifavan and ptr1.
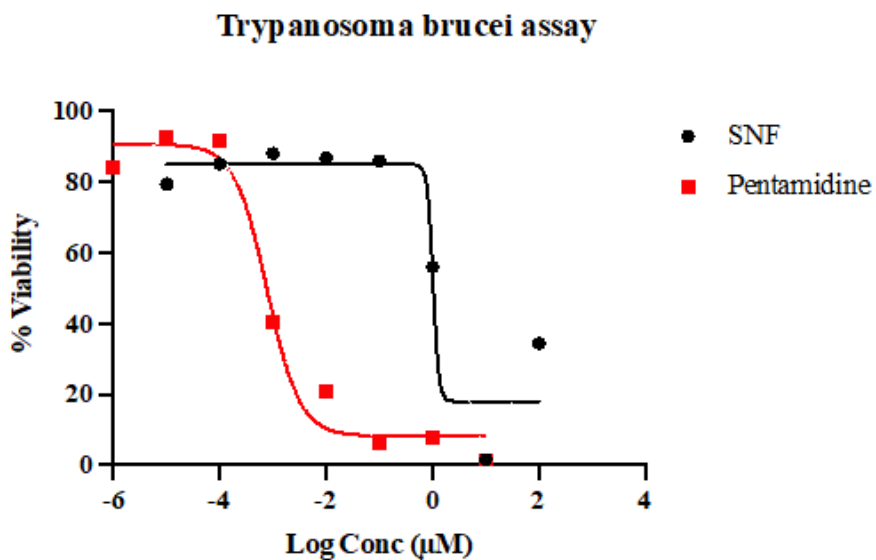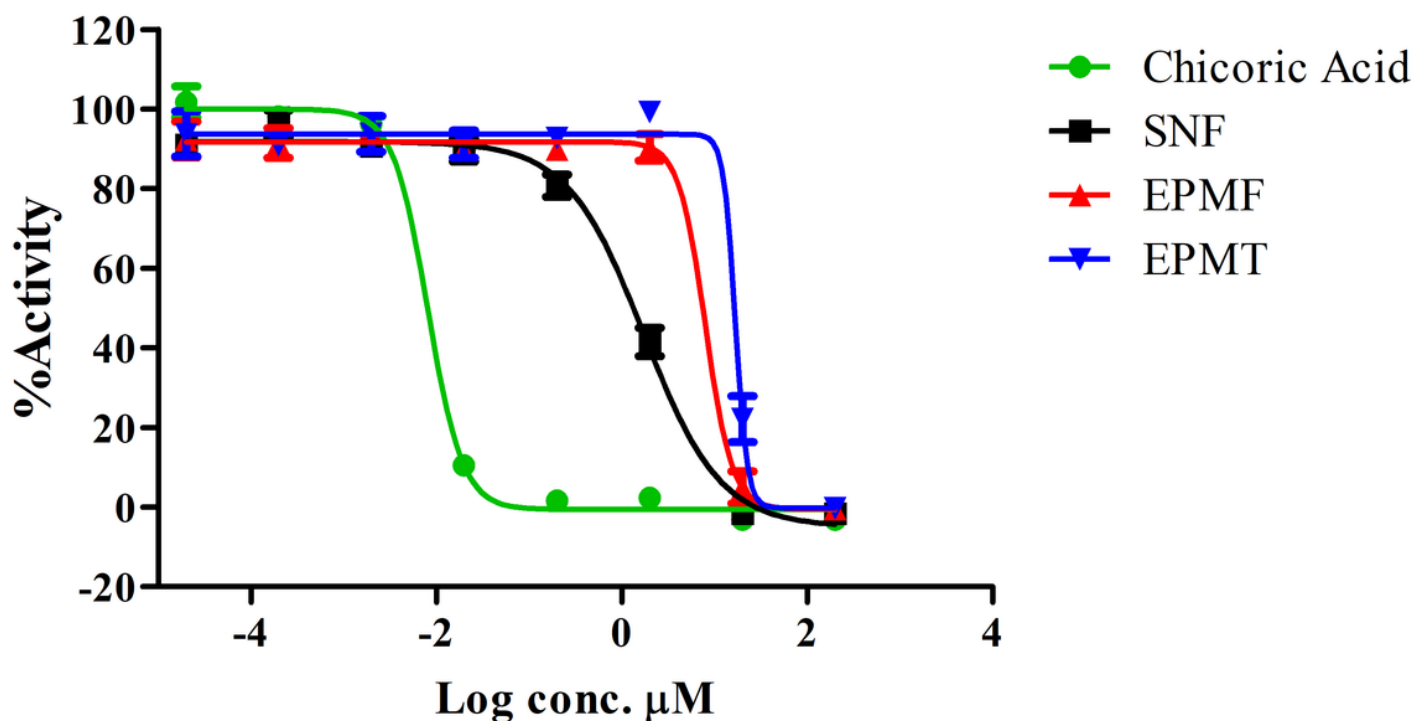

Figure 4

Dose-response curve for trypanosome assay.

Figure 5

The dose−response plots obtained for the extract in an hiv integrase enzyme assay.

The % enzyme activity levels were derived from the absorbance values of the experimental sample compared to the untreated (control) samples. The log[extract] is plotted against the % IN enzyme activity. A non-linear regression analysis was used to calculate the IC_{50} value for the extract. Data manipulation was performed as described in the methodology.

Supplementary Files

This is a list of supplementary files associated with this preprint. Click to download.

- SuppementarymaterialR.docx